Modeling the Orbit and Physical Characteristics of Near Earth Asteroid 2002 UX

J. Brettle, A. Caosun, A. Perea Rojas, T. Tan

August 5, 2018

Abstract

The research conducted on Near Earth Asteroid 283729, also designated 2002 UX, over the course of July 2018 verified the short term orbit model and absolute magnitude published in the JPL HORIZONS Ephemeris, and found the object's albedo, size, and color. The albedo was measured at 0.1 - 0.2 of full reflectivity and the V-R index was calculated to be 0.222 which implied a silicaceous asteroid due to its bluer color relative to the sun. The classical orbital elements determined by this study were
$a = 1.624 \pm 0.110, e = 0.175 \pm 0.0438, i = 26.207 \pm 1.18, \Omega = 266.157 \pm 2.00$, and
$\omega = 66.433 \pm 14.1$. The closest approach 2002 UX will make is 0.279 AU on November 19th, 3805

1. INTRODUCTION

Observing relatively unobserved near earth asteroids expands upon the human tower of knowledge, and predicts the threat level of potentially life-altering collisions. This paper discusses Asteroid 283729, designated 2002 UX. 2002 UX is one of the Amor Asteroids - a group that orbits the sun near Mars and approaches the Earth. As of July of 2018, 2002 UX has only 402 recorded observations. There is little published information regarding the albedo, size, B-V color index, and long-term orbit model of this asteroid. The preliminary orbit model was created using Carl Friedrich Gauss's "Method of Gauss", which utilizes integration, differentiation and vector geometry to transform three initial right ascension, declination, and Julian Day values into an ellipitical orbit. This orbit was then optimized using gradient climbing in the six dimensions of x,y,z and vx,vy,vz in order to reduce the χ value. The vectors from this optimized orbit served as the baseline to predict possible threat from the asteroid and to determine the probable size and albedo ranges.

2. METHODS AND OBSERVATION

2.1 Observations

Over the course of four weeks, images of 2002 UX and the surrounding celestial sky were taken locally with the 16-inch RCOS telescope at the Leitner Observatory in New Haven, Connecticut, and remotely with 20-inch telescope at the Siding Spring Observatory in Coonabarabran, Australia, and the 24-inch telescope at the Sierra Remote Observatory at Auberry, California, through the iTelescope network.

2.1.1 Local Observing

With the astrometric right ascension and declination of 2002 UX from JPL, standard observing preparations and telescope set up procedures were followed. The pictures were then taken with a CCD camera and SkyX software.

All local pictures were taken between 1:00UTC and 6:00UTC to take pictures near transit. The images, along with autodarks for calibration, were originally taken with 1x1 binning, an empty filter, exposures of 60 seconds, and in sets of 5 images. However, during later stages, due to the increasing magnitude of the asteroid, images were taken with exposure times of 90 seconds.

2.1.2 Remote Observing

After 2002 UX had an approximate magnitude of greater than 17.8, it was no longer measurable from the telescopes at Leitner Observatory. Pictures taken from July 21, 2018 onward were done entirely through the remote iTelescope network. These images were taken in sets of 5 with corresponding autodarks and 2x2 binning. Non-filtered pictures had exposure times of 60 seconds that later increased to 90 seconds while pictures taken through the R and V filters consistently had exposure times of 90 seconds.

2.2 Data Processing

2.2.1 Asteroid Detection

The first sets of images were aligned and compared to find the asteroid among other celestial objects. However, as 2002 UX became progressively fainter, the solve-field technique from astrometry.net proved more efficient. This technique would match stars in the image with measured star maps, and the image and coordinate map would be opened with DS9. As a result, the astrometric coordinates of 2002 UX from JPL were highlighted as pixel values in the image, and blinking determined whether the object located in the highlighted area traveled in the expected trajectory of 2002 UX.

2.2.2 Determination of Right ascension, Declination, and Apparent Magnitude

The World Coordinate System within the solve-field method and the UCAC4 catalog in DS9 were used to find the right ascension and declination of the pixels of each image. The centroid coordinates from the light distribution of the asteroid were used as an input for finding the celestial coordinates on the image map. In addition, with the UCAC4 catalog, a star with known magnitude that was close to the asteroid in the image was used to calibrate the magnitudes in the Maxim DL tool to find the brightness of the asteroid.

2.2.3 Albedo [1] [2]

Due to the dim magnitude of 2002 UX and the greater light gathering power of remote telescopes, V and R filtered images were taken only during remote observation but were calibrated in the same manner that was used to determine apparent magnitude as described above. However, due to the differences between the V-R indices from the database and the calibrated V-R indices from the picture, the linear relationship was determined through 8 different stars and the resulting line from least squares regression was used to find the actual V-R value of the asteroid. This updated V minus R value was then compared to that of the Sun, as an asteroid has no inherent brightness and all of its color values were reflected from the Sun. The albedo was measured using the fraction of total light reflected based off of its probable asteroid categorization due to its apparent color index value where. If the color index was within 0.1 of the V-R color index of the Sun (0.352) then it was categorized as a C type asteroid and given a probable range of albedo of .02 to .05, while if it was not within that range, it was categorized as an S type asteroid and given a probable albedo range of 0.1-0.2.

2.2.4 Preliminary Orbit Determination [3] [4]

The preliminary orbit was determined by using the method of Gauss to find the position $\vec{r}$ and velocity $\dot{\vec{r}}$ of the asteroid at a certain time. The Method of Gauss takes the right ascension, declination, and Julian Day of three observations along with a random guess of $|\vec{r}|$ for the middle observation.

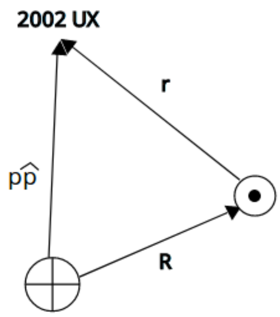

Figure 1: Diagram of 2002 UX, Earth, and Sun positions and vector designations.

The Method of Gauss requires three separate observations of the position of the Sun with respect to the Earth, $\vec{R}_i$, and the position unit vector of 2002 UX with respect to the Earth, $\hat{\rho}_i$. $\vec{R}_i$ was determined using the Ephemeris DE421 while $\hat{\rho}_i$ was determined using the measurements from three different nights.

$$\hat{\rho} = \cos\alpha\cos\delta\hat{x} + \sin\alpha\cos\delta\hat{y} + \sin\delta\hat{z}$$

The JPL Ephemeris produces vectors using the center of the Earth instead of the position of the observer. As such, parallax was corrected for in $\vec{R}$ with g, a vector from the center of the Earth to the observer's position:

$$g = R_e\big[\cos(LST)\cos(lat)\hat{x} + \sin(LST)\cos(lat)\hat{y} + \sin(lat)\hat{z}\big]$$

$$\vec{R}_{topo} = \vec{R}_{geo} - \vec{g}$$

The f and g series, derived from a Taylor expansion, were then used to determine ρ_i.
Sun-to-asteroid $\vec{r}$ was estimated using $|\rho|\hat{p}$ and $\vec{R}$. The $\dot{\vec{r}}$ is then determined using the previous data and the $\vec{r}$ in the first and last times inputted. $\vec{r}$.

This process is then iterated 50 times with the previous output of r as the new guess for $|\vec{r}|$ or until ρ_i are consistent. The r_i and $\dot{r}_i$ are then rotated from equatorial to ecliptic, and the orbital elements (angular momentum h, eccentricity e, perihelion distance q, and semi-major axis a) are determined.

2.2.5 Ephemeris Generation [5]

An Ephemeris Generation technique was utilized to check for errors and calculate residuals of the $\vec{r}$ and $\dot{\vec{r}}$ determined from the preliminary orbit generation. With this technique, the same vector triangle of $\vec{r}$, $\vec{\rho}$, and $\vec{R}$ (shown in Fig. 1) with the same topographic correction was reversed after integrating the time forward using Störmer-Verlet Integration.

2.2.6 Orbit Optimization [6]

The preliminary orbit was optimized by iterating to find lower residuals using two three-dimensional vectors randomized by a simple Gaussian distribution where the middle was anchored at the current χ value. Due to the necessity of minimizing both the residuals from the right ascension and the declination, the χ value was defined as

$$\chi = \sqrt{\left(\sum Residuals_{RA}\right)^2 + \left(\sum Residuals_{DEC}\right)^2}$$

An iterized addition of randomized three dimensional vectors to the current $\vec{r}$ and $\dot{\vec{r}}$ was incorporated with the ephemeris generation to recalculate the right ascension and declination for each time in the observations. This eventually returned a new chi value which was then compared to the current best chi value; if better, the current iteration was replaced with the newly changed $\vec{r}$ and $\dot{\vec{r}}$.

2.2.7 Magnitude and Size

The removal of the distance's influence on the apparent magnitude of 2002 UX produced the reduced magnitude of the asteroid.

$$H(\alpha) = V - 5log(r\rho)$$

The angle between $|\rho|\hat{\rho}$ and $\vec{r}$, phase angle, and the apparent magnitude are then used to determine the absolute magnitude of the asteroid.

$$H = H(\alpha) + 2.5\log(.85)^{3.33\tan(\alpha)^{.315}} + .15^{1.87\tan(\alpha)^{.61}}$$

The diameter of the asteroid is determined with its albedo and absolute magnitude.

$$D = 10^{3.1236-0.5\log(albedo)-0.2H(\alpha)}$$

2.2.8 Long-term Orbit Integration

Over long periods of time, the Störmer-Verlet Integration method accumulates a large amount of error. Instead REBOUND's N-Body integration software for the purpose of gravitational modeling - was used for our long-term orbit integration. With a starting position and velocity found using the methods in section 2.2.6, the orbit of 2002 UX was integrated over 10^5 years.

3. RESULTS

3.1 Sample Images

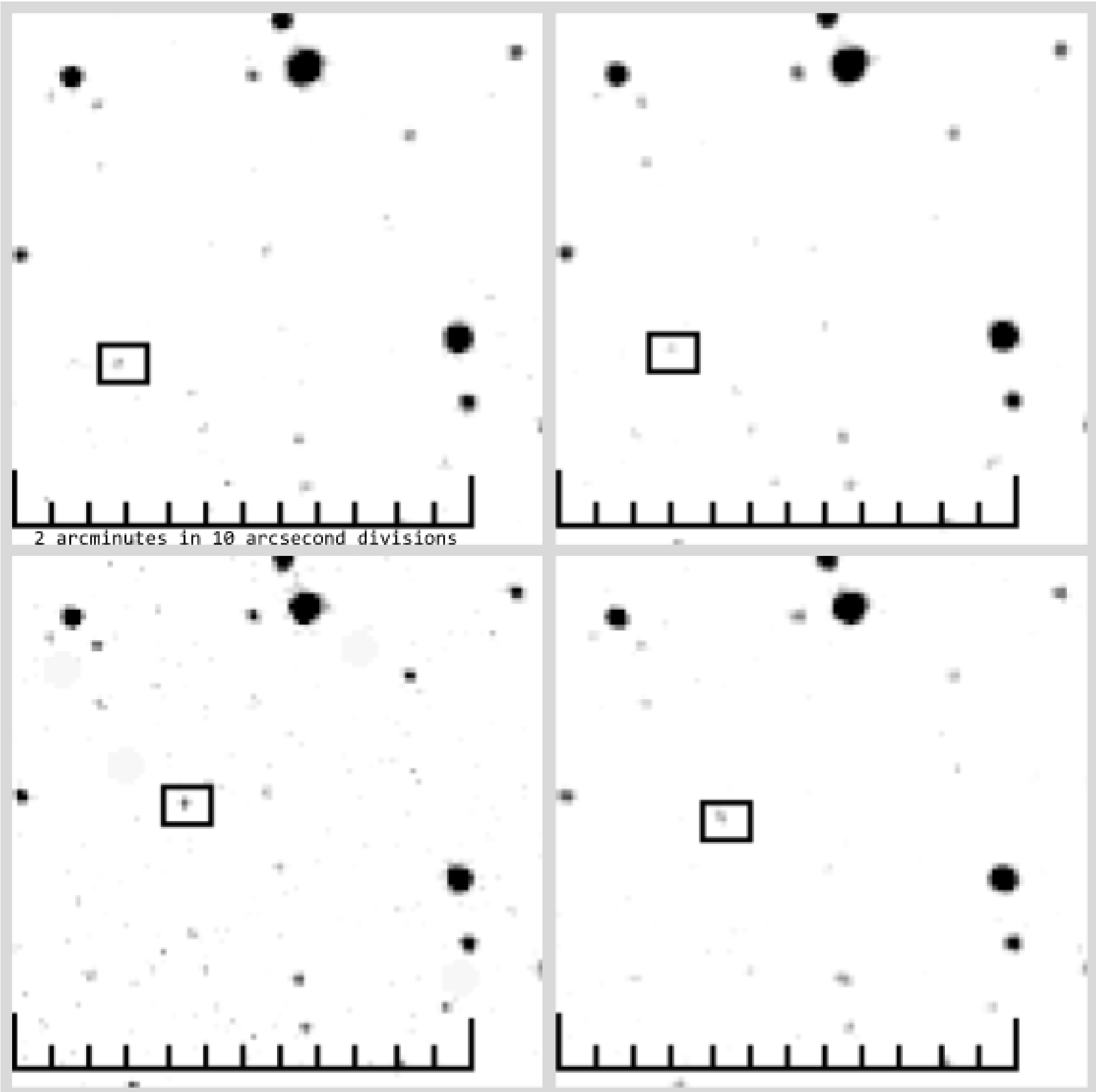

Figure 2: Images taken from Leitner Observatory on 12 July 2018 of RA 18h 12m 49.81s Dec 07 deg 01' 43.07" with 2002 UX marked by rectangle.

3.2 Tables, Graphs and Figures

JPL Predicted Values for RA, DEC, and MAG vs, Observed Values - Julian Day and decimal degree

DATE (JD)	RA(Obs)	RA(JPL)	DEC(Obs)	DEC(JPL)	MAG(Obs)	MAG(JPL)
2458311.686	273.2075	273.20750	7.01694	07.016944	17.4	17.45
2458311.698	273.2027	273.20208	7.03389	07.033889	17.4	17.45
2458313.044	272.6462	272.64625	7.99972	07.999722	17.5	17.50
2458313.056	272.6411	272.64100	8.00000	08.000000	17.5	17.50
2458313.068	272.6356	272.63575	8.00000	08.000000	17.5	17.50
2458317.052	271.1053	271.10529	10.61000	10.610000	17.7	17.65
2458317.066	271.0998	271.09971	10.62694	10.626944	17.7	17.65
2458317.086	271.0915	271.09167	10.62694	10.626944	17.7	17.65
2458317.659	270.5444	270.88967	11.55917	10.982778	17.6	17.63
2458317.671	270.5400	270.88508	11.57611	10.982778	17.6	17.63
2458317.691	270.5329	270.87750	11.57611	10.999722	17.6	17.63
2458320.584	269.9205	269.92096	12.64389	12.643889	17.7	17.75
2458320.587	269.9198	269.92000	12.64389	12.643889	17.7	17.75
2458320.590	269.9187	269.91883	12.64389	12.643889	17.7	17.75
2458320.835	269.8393	269.83929	12.77944	12.779444	17.8	17.76
2458320.845	269.8360	269.83587	12.79639	12.796389	17.8	17.76
2458320.853	269.8332	269.83317	12.79639	12.796389	17.8	17.76

Table I: Observed results of right ascension and declination compared to accepted values from JPL Horizons. [7]

Classical Orbital Elements		
	Calculated Value	Horizons
a	1.624 ± 0.110	1.4732
e	0.175 ± 0.0438	.164
i	26.207 ± 1.18	20.206
Ω	266.157 ± 2.00	263.867
ω	66.433 ± 14.1	84.33

Table II: Calculated results compared to accepted JPL Horizons values. The calculated values are derived using the output $\vec{r}$ and $\dot{\vec{r}}$ from the method of gauss on July 17th 2018 at 13:14:53.

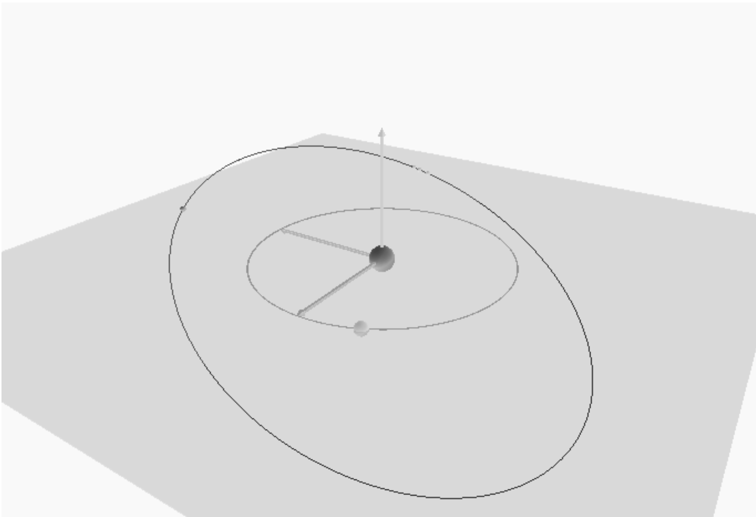

Figure 3: Visualization of the orbit of 2002 UX using VPython. (The outside curve is the orbit of the asteroid, the sphere in the center is the Sun and the inside curve is the orbit of the Earth, the plane represents the ecliptic plane). The three circled spheres indicate the position of the asteroid during the 3 calibration times in method of Gauss used to create the preliminary orbit.

3.3 Data Analysis 3.3.1 Right Ascension, Declination and Magnitude data

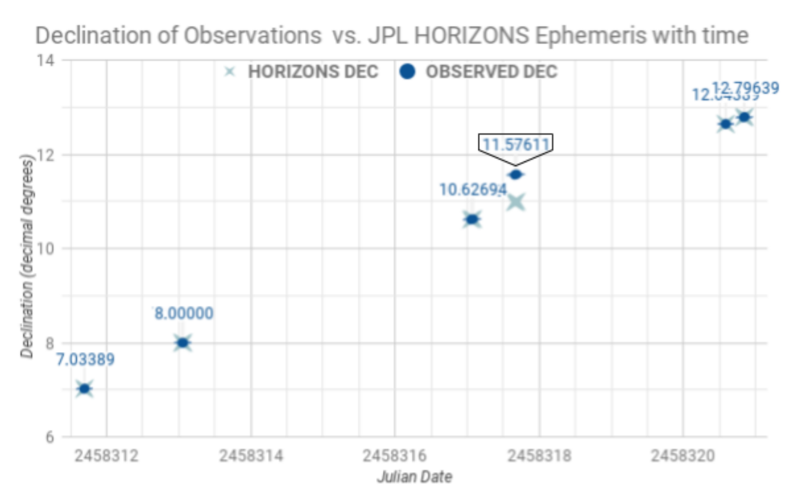

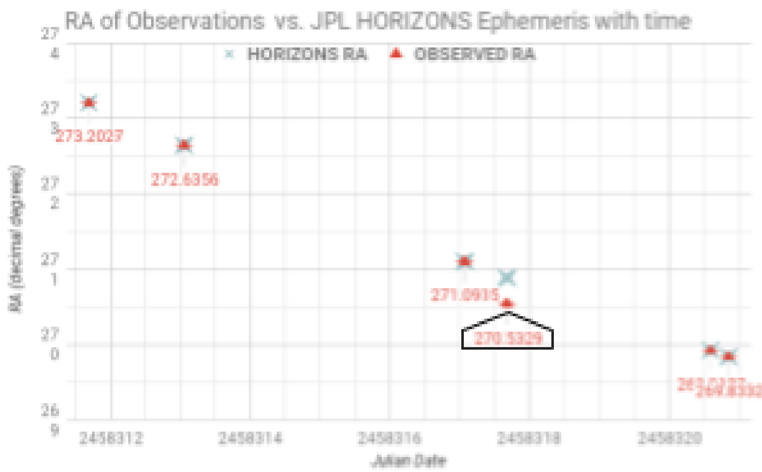

Figure 4 and Figure 5: Graphs depicting the differences in right ascension and Magnitude between the observed values and the accepted values. The anomalous night is distinguished by the black figure. The uncertainty is approximately $\pm .0024053°$.

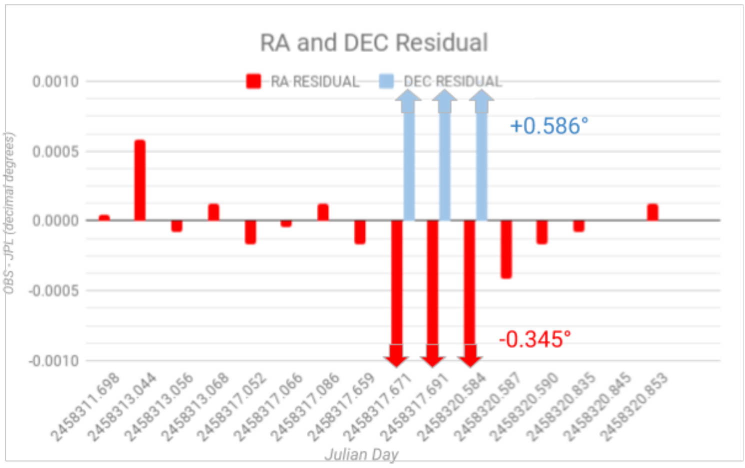

Figure 6: Visualization of the residuals between the observed and accepted values of right ascension and declination across the various days of observation. (Note that on most of the days, the declination difference is approximately 0, and therefore does not appear on the graph)

Utilizing the techniques mentioned above resulted in the measurements for right ascension, declination, and magnitude of 2002 UX. All except one night of measurements deviated in a range of 1-3 arc seconds away from the accepted JPL Horizons value. Unaccounted perturbations from another celestial body could be the cause behind the measurements on the anomalous night or the measurements could belong to a different asteroid. Nevertheless, the data from that night was ignored while calibrating orbit optimization as its effect would have overwhelmed the significance of the residuals of the other 14 measurements.

Furthermore, a χ^2 Goodness of Fit test was performed on the measurements compared to the JPL expected values. The right ascension, declination, and magnitude χ^2 statistics were 0.00132, 0.0925, and 0.00141 respectively. With a P-value of .99, the results prove no significant difference, and the observations follow the expected distribution.

3.3.2 Measured Orbital Elements
After orbit optimization, the $\vec{r}$ and $\dot{\vec{r}}$ equated to the following.

$$\vec{r} = 0.433\hat{x} - 1.29\hat{y} - 0.281\hat{z}$$

$$\dot{\vec{r}} = 0.732\hat{x} + 0.236\hat{y} + 0.479$$

These values were then contorted to equate the base values of the classical orbital elements. The contortion of the values are explained with greater detail in the Appendix. Moreover, because method of Gauss was used as the primary method of orbit determination, the uncertainties were found through the Monte Carlo Method. The formulas found in the appendix were applied to 1000 $\vec{r}$ and $\vec{r}$ found by adding a small randomized 3 dimensional vector to both values, and then finding the standard deviation of the 1000 orbits. Moreover, the χ^2 goodness of fit statistic of the orbital elements is 1.804. With a P-value of 0.771787, the orbital elements are not significantly different from the predicted values of JPL Horizons.

3.3.3 Color Index, Albedo and Size [2] [1]

V-R Color Index Calibration

Source	V (UCAC)	v (Image)	R (UCAC)	r (Image)	V-R (UCAC)	v-r (Image)
Callibration Star	14.4110	-	14.1670	-	-	-
LS Star 1	13.6500	13.6330	13.2670	13.2330	0.3830	0.4000
LS Star 2	15.0860	15.1290	14.8650	14.9010	0.2210	0.2280
LS Star 3	14.3690	14.3750	13.9960	14.0160	0.3730	0.3590
LS Star 4	13.8520	13.9230	13.6100	13.6960	0.2420	0.2270
LS Star 5	13.8760	13.9570	13.7230	13.7930	0.1530	0.1640
LS Star 6	12.1460	12.1740	11.7380	11.7730	0.4080	0.4010
LS Star 7	14.8690	14.9700	14.5890	14.6940	0.2800	0.2760
LS Star 8	14.5470	14.5720	14.2670	14.4370	0.2800	0.1350
Asteroid	-	17.9330	-	17.7540	0.2222	0.1790

Table III: The color magnitude values for 8 stars around 2002 UX in both the image, which is calibrated using a calibration star, and the database.

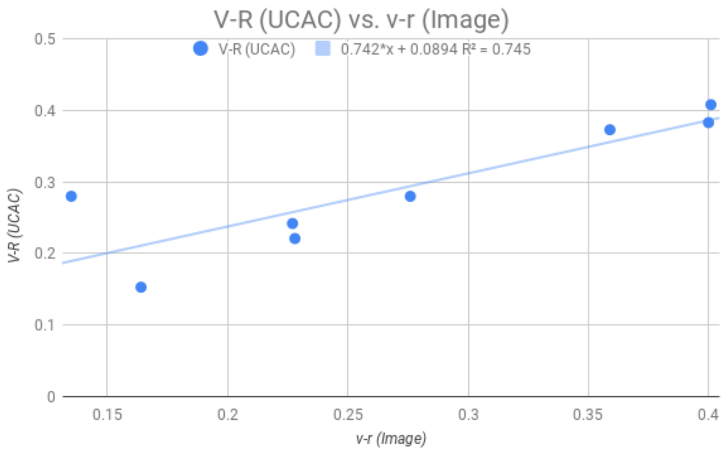

Figure 7: The line of best fit relating the v-r index from the image to the accepted V-R values used to find the actual V-R value of the asteroid.

Using the line of best fit and the v-r (image) of 0.176, the actual V-R color index of 2002 UX came out to be .222218. Since this is within ± 0.1 of the V-R color index of the Sun, this means that 2002 UX is most probably an S type asteroid meaning that its albedo is within the range of 0.1-0.2. Using the calculations from above, this means that 2002 UX has a diameter of 0.666 km to 0.941 km.

3.3.4 Long-term Integration and Threat

Using the REBOUND integrator, it was found that the closest approach within 2000 years occurred on November 19th, 3805, at a distance of 0.326AU. The closest approach of 2002 UX to Earth within the span of 100000 years occurred 20285.2 years after July 17th, 2018, at a distance of 0.279AU. Within the first 20285.2 years, the asteroid slowly and consistently crept closer to Earth, but started moving farther away afterwards. Furthermore, with the Monte Carlo method, using a cloud of 200 asteroids, no asteroid ever came closer than 0.311AU within 1000 years. As such, 2002 UX has a very low probability of impact.

4. CONCLUSION

As seen in Table I, other than the unused set of images - those taken on July 18th - the measured right ascensions and declinations were within a few arcseconds of JPL's predictions. Furthermore, when the optimized position and velocity vectors from 2.2.6 were put into an integrator, they modeled the measured RA and Dec more closely than the vectors from JPL. This may be because JPL's Ephemeris generation comes from the year 2013; Between 2013 and 2018, another celestial body could have caused perturbations in the orbit of 2002 UX. This implies that the measured data and resulting orbit model is more accurate than previously predicted orbits. From our long-term integration and Monte Carlo method, we found that within the next 100000 years, the asteroid's closest approach to the Earth occurs at a distance of 0.279AU. As such, 2002 UX will not pose a threat to Earth in the near future. However, when the optimized vectors were used to calculate orbital elements, even small changes in either vector produced drastic differences in the resulting eccentricity, ranging from low values of 0.02 to non-orbital values of 2.5. Though a consistent value of 0.17 was found later, it is clear that more precise values and better orbit models are required to accurately model the motion of 2002 UX. This could be achieved with a telescope with more light gathering power, leading to lower uncertainty in right ascension and declination measurements. Furthermore, faster computers would allow us to easily run more complex and complete orbit models. If implemented, these changes would improve our data collection and resulting analysis, especially our orbit predictions.

ACKNOWLEDGMENTS

This research project was accommodated for by the Yale Summer Program in Astrophysics. This project would not have been possible without the multiple efforts of the YSPA staff. Firstly the help from Dr. Michael Faison for starting this amazing program, for his amazing lectures, and for his overwhelming helpful presence during the program. Additionally, thanks need to be distributed to Dr. Fallscheer for her entertaining yet informative lectures and help with observations, and Ms. Kimberly Nucifora for her overwhelming warmth and commitment to this program. Finally this paper would not have become a reality without the T.A's, Clare Staib-Kaufman and Daniel Heimsoth for their willingness to answer the variety of absurd and curious questions asked by students. Thank you.

References

[1] B. A. Assoc, “The h and g magnitude system for asteroids.”

[2] JPL, “Asteroid size estimator.”

[3] D. M. Faison, “Angles-only orbit determination from three observations: Method of gauss.”

[4] D. M. Faison, “Numerical integration with the f and g series.”

[5] D. M. Faison, “Ephemeris generation using the jpl de421 solar system ephermeris.”

[6] D. M. Faison, “Numerical integration.”

[7] JPL, “Jpl horizons.”

APPENDIX

JPL Predicted Values for RA, DEC, and MAG vs, Observed Values - UTC Date and Sexagesimal

DATE	RA(Obs)	RA(JPL)	DEC(Obs)	DEC(JPL)	MAG(Obs)	MAG(JPL)
2018 07 12.18592	18 12 49.81	18 12 49.80	07 01 43.07	07 01 42.8	17.4	17.45
2018 07 12.19791	18 12 48.64	18 12 48.50	07 02 13.04	07 02 13.7	17.4	17.45
2018 07 13.54377	18 10 35.08	18 10 35.10	07 59 36.08	07 59 36.5	17.5	17.50
2018 07 13.55563	18 10 33.87	18 10 33.84	08 00 06.05	08 00 06.0	17.5	17.50
2018 07 13.56750	18 10 32.54	18 10 32.58	08 00 35.07	08 00 35.5	17.5	17.50
2018 07 17.55182	18 04 25.26	18 04 25.27	10 36 36.09	10 36 37.1	17.7	17.63
2018 07 17.56601	18 04 23.96	18 04 23.93	10 37 08.02	10 37 08.3	17.7	17.63
2018 07 17.58640	18 04 21.96	18 04 22.00	10 37 53.04	10 37 53.1	17.7	17.63
2018 07 18.15876	18 02 10.65	18 03 33.52	11 33 43.07	10 58 15.7	17.6	17.65
2018 07 18.17074	18 02 09.59	18 03 32.42	11 34 08.01	10 58 41.6	17.6	17.65
2018 07 18.19067	18 02 07.90	18 03 30.60	11 34 49.08	10 59 24.6	17.6	17.65
2018 07 21.08397	17 59 40.93	17 59 41.03	12 38 39.04	12 38 36.5	17.7	17.75
2018 07 21.08669	17 59 40.76	17 59 40.80	12 38 44.06	12 38 41.9	17.7	17.75
2018 07 21.09017	17 59 40.50	17 59 40.52	12 38 49.09	12 38 48.7	17.7	17.75
2018 07 21.33524	17 59 21.43	17 59 21.43	12 46 45.09	12 46 46.2	17.8	17.76
2018 07 21.34539	17 59 20.64	17 59 20.61	12 47 05.06	12 47 05.7	17.8	17.76
2018 07 21.35346	17 59 19.96	17 59 19.96	12 47 21.03	12 47 21.1	17.8	17.76

Table IV: Raw data submitted to the minor planet center in decimal days, hours, and degrees.

Newton's Law of Gravitation and the vector triangle in Figure 1 form the basis for the Method of Gauss:

$$\ddot{\vec{r}} = \frac{-\mu\vec{r}}{r^3}$$

$$\vec{r} = \rho\hat{\rho} - \vec{R}$$

where $\ddot{\vec{r}}$ denotes acceleration and μ denotes the mass of the sun. All other terms are defined in Figure 1. Next, the f and g series from the Taylor expansion are found:

$$r(\tau) = r_2 + \dot{\vec{r}}_2\tau - \frac{\vec{r}_2}{2r_2^3}\tau^2 - \frac{\dot{\vec{r}}_2}{6r_0^3}\tau^3$$

$$r(\tau) = f_\tau\vec{r}_2 + g_\tau\dot{\vec{r}}_2$$

$$f_\tau = 1 - \frac{1}{2r_0^3}\tau^2...$$

$$g_\tau = \tau - \frac{1}{6r_0^3}\tau^3...$$

where τ is the time step of integration. a_1 and a_3 are calculated by:

$$a_1 = \frac{g_3}{f_1g_3 - f_3g_1}$$

$$a_3 = \frac{g_1}{f_1g_3 - f_3g_1}$$

Using these, ρ_i is found:

$$\rho_1 = \frac{a_1(R_1 \times \hat{\rho}_2) \cdot \hat{\rho}_3 - (R_2 \times \hat{\rho}_2) \cdot \hat{\rho}_3 + a_3(R_3 \times \hat{\rho}_2) \cdot \hat{\rho}_3}{a_1(\hat{\rho}_1 \times \hat{\rho}_2) \cdot \hat{\rho}_3}$$

$$\rho_2 = \frac{a_1(\hat{\rho}_1 \times R_1) \cdot \hat{\rho}_3 - (\hat{\rho}_1 \times R_2) \cdot \hat{\rho}_3 + a_3(\hat{\rho}_1 \times R_3) \cdot \hat{\rho}_3}{-(\hat{\rho}_1 \times \hat{\rho}_2) \cdot \hat{\rho}_3}$$

$$\rho_3 = \frac{a_1(\hat{\rho}_2 \times R_1)\cdot\hat{\rho}_1 - (\hat{\rho}_2 \times R_2)\cdot\hat{\rho}_1 + a_3(\hat{\rho}_2 \times R_3)\cdot\hat{\rho}_1}{a_3(\hat{\rho}_2 \times \hat{\rho}_3)\cdot\hat{\rho}_1}$$

An initial guess for the value of $\vec{r}_2$ is required for a_1 and a_3 to integrate. The distance to the asteroid, ρ_2, is measured, and using the vector triangle, another value of $\vec{r}_2$ is input into the process. This is repeated until the input value of $\vec{r}_2$ converges with the output value. Then, $\dot{\vec{r}}_2$ can be found with:

$$\dot{\vec{r}}_2 = \frac{f_3}{g_1 f_3 - g_3 f_1} r_1 - \frac{f_1}{g_1 f_3 - g_3 f_1} r_3$$

where r_1 and r_3 are found using ρ_1, ρ_3, and the vector triangle.
Finally, with $\vec{r}_2$ and $\dot{\vec{r}}_2$, the classical orbital elements can be determined. The following equations were used to find $\vec{h}$, angular momentum; e, eccentricity; a, semimajor axis; q, perihelion distance; i, inclination; $\vec{N}$, direction of the ascending node; Ω, longitude of the ascending node; and ω, argument of the perihelion.

$$\text{Angular Momentum: } \vec{h} = \vec{r} \times \dot{\vec{r}}$$

$$\text{Eccentricity: } \vec{e} = \frac{\dot{\vec{r}} \times \vec{h}}{\mu} - \hat{r}$$

$$\text{Semimajor Axis: } a = \frac{h^2}{\mu(1-e^2)}$$

$$\text{Perihelion Distance: } q = a(1-e)$$

$$\text{Inclination: hcos}(i) = \vec{h}\cdot\hat{z}$$

$$\text{Direction of the Ascending Node: } \vec{N} = \hat{z} \times \vec{h}$$

$$\text{Longitude of the Ascending Node: } \cos(\Omega) = \hat{x}\cdot\hat{N}$$

$$\text{Argument of the Perihelion: } \cos(\omega) = \hat{e}\cdot\hat{N}$$

-1 Formatting: Julia Brettle
0 Abstract: Julia Brettle
1 Introduction: Julia Brettle, Tony Tan
2 Methods and Observations:
2.1 Observations:
2.1.1 Local Observing: Alejandra Perea and Andrew Caosun
2.1.2 Remote Observing: Alejandra Perea and Andrew Caosun
2.2 Data Processing:
2.2.1 Asteroid Detection: Alejandra Perea
2.2.2 Determination of Right Ascension, Declination, and Apparent Magnitude: Alejandra Perea
2.2.3 Albedo: Alejandra Perea and Tony Tan
2.2.4 Preliminary Orbit Determination: Alejandra Perea and Tony Tan
2.2.5 Ephemeris Generation: Tony Tan
2.2.6 Orbit Optimization: Tony Tan
2.2.7 Magnitude and Size: Alejandra Perea
2.2.8 Long-term Integration: Andrew Caosun
3 Results:
3.1 Sample Images: Julia Brettle
3.2 Tables, Graphs, and Figures: Tony Tan and Julia Brettle
3.3 Data Analysis:
3.3.1 Right Ascension, Declination, and Magnitude: Tony Tan
3.3.2 Measured Orbital Elements: Tony Tan
3.3.3 Color Index, Albedo, and Size: Tony Tan
3.3.4 Long-term Integration and Threat: Andrew Caosun
4 Conclusion: Andrew Caosun
5 Acknowledgements: Alejandra Perea
6 References: Tony Tan
7 Appendix: Andrew Caosun